American Journal of Science, Engineering and Technology
2022; 7(3): 87-91
http://www.sciencepublishinggroup.com/j/ajset
doi: 10.11648/j.ajset.20220703.14
ISSN: 2578-8345 (Print); ISSN: 2578-8353 (Online)

Study of Microstructure and Properties of Gold Based Brush Materials

Xiumei Shi[1, 2], Lei Jiao[2, 3], Feng Wang[2, 4], Richu Wang[1], Xu Liu[2, 3], Yuefeng Qi[2, 3]

[1]School of Materials Science and Engineering, Central South University, Changsha, China
[2]Beijing Non-ferrous Metals and Rare Earth Research Institute Co., Ltd., Beijing, China
[3]Beijing Engineering Research Center of New Brazing Materials for Electronic Information, Beijing, China
[4]School of Materials Science and Engineering, University of Science and Technology Beijing, Beijing, China

Email address:
6918541@qq.com (Xiumei Shi)

To cite this article:
Xiumei Shi, Lei Jiao, Feng Wang, Richu Wang, Xu Liu, Yuefeng Qi. Study of Microstructure and Properties of Gold Based Brush Materials. *American Journal of Science, Engineering and Technology*. Vol. 7, No. 3, 2022, pp. 87-91. doi: 10.11648/j.ajset.20220703.14

Received: July 3, 2022; **Accepted**: July 28, 2022; **Published**: August 15, 2022

Abstract: Electric brushes for aerospace vehicles—conductive rings electrically contact sliding friction pairs, are important power and signal transmission channels for aerospace vehicles. They are key stand-alone products that affect the life and reliability of satellites. In addition to ensuring high reliability in structure, friction pair materials should also select electrical contact materials suitable for space environment. This paper studies the corresponding relationship among the process, performance and organization of AuNi9 brush wire as one of the sliding friction pairs, especially for the process link of key performance changes. AuNi9 alloy was prepared and investigated in order to obtain excellent mechanical properties by optimizing the heat treatment conditions in this paper. The results show that the microstructures of the alloy are mainly composed of α-Au solid solution and A small amount of Au-Ni phase. The strength and hardness of the material continue to increase with the increase of deformation rate, and the strength is basically linear. However, the hardness has a limit value, and even if the deformation rate continues to increase, the hardness does not change significantly. The AuNi9 alloy has obvious aging strengthening phenomenon. When the temperature is kept at 300°C, the hardness increases with the heat treatment. The optimal heat treatment process of AuNi9 alloy is heating at 300°C for 30 minutes.

Keywords: Noble Metal, Sliding Friction Pair, Brush Wire, Microstructure, Properties

1. Introduction

With the development of science and technology, aerospace technology has been gradually applied in satellite positioning, long-distance communication, space exploration, resource exploration and other fields, and has an irreplaceable role in national defense and people's livelihood [1, 2]. Space vehicles mainly rely on solar panels to collect solar energy and convert electrical energy for battery life. Therefore, solar panels are very important for a space vehicle and known as heavy equipment [3, 4]. The solar panel drive mechanism is used to drive the rotation of the spacecraft solar panel, realize the sun orientation of the solar cell array, enable the satellite to obtain as much energy as possible, and provide a power and signal transmission channel between the spacecraft body and the solar panel [5]. It is a key stand-alone product that affects the life and reliability of satellites [6]. The driving mechanism of the solar panel is mainly composed of conductive friction pairs. The conductive friction pair provides continuous long-term signal and power transmission in vacuum for spacecraft, satellites, manned spacecraft, manned space stations and other spacecraft [7]. The electrical contact material for the space environment should be selected for the brush slip ring system to achieve this function [8]. The electrical contact friction pair of the device is required to have small and stable contact resistance for achieving high reliability and long service life. Hence, good wear resistance and low friction coefficient of the electrical contact friction pair materials are necessary [9].

The sliding interface of the brush needs to transmit the current, which makes the wear state of the brush more complicated than the general wear. Lot of Joule heat is generated in the brush wire during the reciprocating sliding

process due to the existence of the current. The microstructure of the contact materials is changed under the influence of the Joule heat. The wear failures such as adhesion wear, abrasive wear, fatigue fracture and vibration wear occur after a series of solidification, hardening, corrosion, melting processes [10]. Wang et al. [11]. investigated the friction and wear behavior of AuNi9/Au coating tribo-couple under different loads, as well as the characteristics of worn surface and wear debris. Li [12] prepared PtIr25 alloy with excellent and stable properties by medium-frequency and high-frequency melting, heat-treatment technology and hot rolling. The microstructure, physical property, mechanical property and electrical property of PtIr25 were studied. Ueno et al. [13] examined the relation between surface roughness condition and contact voltage drop for sliding contacts. It is confirmed that the contact voltage drop is changed by various surface roughness of sliding materials and the real contact area affects the contact voltage drop change. However, the preparation process of AuNi9 and the corresponding relationship between the preparation process, material properties and microstructure have not been studied.

In this paper, AuNi9 alloy was prepared and investigated in order to obtain excellent mechanical properties by optimizing the heat treatment conditions. In addition, the effects of deformation rate on the tensile strength and microhardness were discussed.

2. Experiments

2.1. Melting and Casting

Melting and casting of Au-Ni alloy was made in vacuum induction melting under dynamic argon atmosphere. The targeted composition for melt was Au-Ni (9±0.5). After cleaning with acetone, high purity Au and Ni ingots of 99.999% purity were charged in the Al_2O_3 crucible. Melting was done under inert atmosphere by first evacuating the furnace to 0.001 mbar and then by purging with argon. After holding for a determined time period, the melt was cast into a steel mold. Table 1 shows the chemical composition of AuNi9 alloy obtained in this work.

Table 1. *Chemical composition of AuNi9 alloy obtained in this work (wt%).*

Alloy	Ni	Au
AuNi9	9.1	Bal.

2.2. Secondary Processing

The casting rod was processed into Φ0.5 mm wire with a total deformation rate of 98% subsequently.

The Au-Ni phase diagram is shown in Figure 1 [14]. According to Figure 1, it can be seen that Au-Ni alloy has a broad immiscibility zone in solid state below 812°C. In the low temperature region, the single-phase solid solution decomposes into a two-phase region with an asymmetric solid solubility curve, and there is an amplitude modulation decomposition in the two-phase region. The intermediate annealing cycle was conducted at 300°C for 30 min. Samples for mechanical properties evaluation were prepared with heat treatments at 200°C, 300°C, 400°C and 500°C for 1h after drawing. To explore the impact of holding time on hardness of AuNi9 alloy, samples were also prepared with heat treatments at 300°C for 15 min, 30 min, 60 min and 120 min.

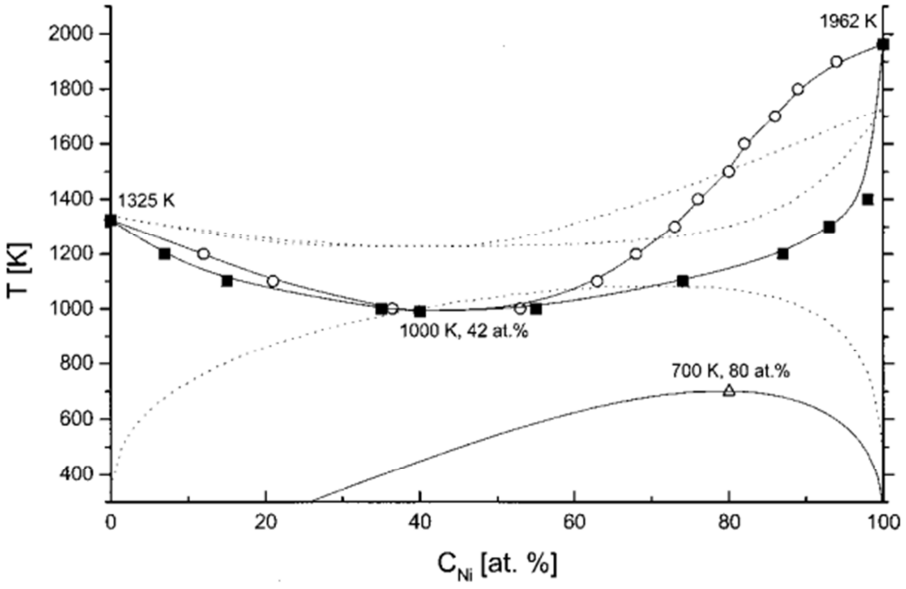

Figure 1. *Phase diagram of Au-Ni alloy.*

2.3. Characterization

The microstructure was observed by metallographic microscope (Observer A1) and scanning electron microscopy (SEM, Hitachi SU-1510). The metallographically prepared samples were etched with the mixed solution as follows: 10ml 68% nitric acid, 50ml 37% concentrated hydrochloric acid and 60ml pure water. An energy dispersive spectroscope (EDS)

was also adopted to determine element composition of the microstructural characteristics and element distribution. Vickers hardness was measured using a 100 g load and a 15 s loading time (Micromet 2100, Buehler). The tensile tests were carried out using a universal testing machine (CMT4105) to investigate the tensile properties of the alloy. The loading speed was 0.5 mm/min. Three specimens were used for each test and the average value was taken into account.

3. Results and Discussion

3.1. Microstructures of AuNi9 Alloy

Figure 2 displays a metallographic picture of AuNi9 alloy. The obvious dendrite structure can be seen in the as-cast structure as given in Figure 2(a). The grain size is small and relatively consistent. The microstructure of as-processed AuNi9 alloy is shown in Figure 2(b).

The deforming twin is observed obviously and increases with the increase in deformation rate. This is because the twin deformation becomes to the main deformation form after the deformation rate reaches to a certain level. The internal organization of the material changes with the processing and heat treatment. The orientation of the grains has changed due to processing. However, there are still some continuous solid solutions after vacuum heat treatment, as shown in Figure 2(c). The dislocation glide is hindered due to the heat-treated structure made up of twinning and Discontinuous solid solution, and hardness and strength increases while elongation decreases.

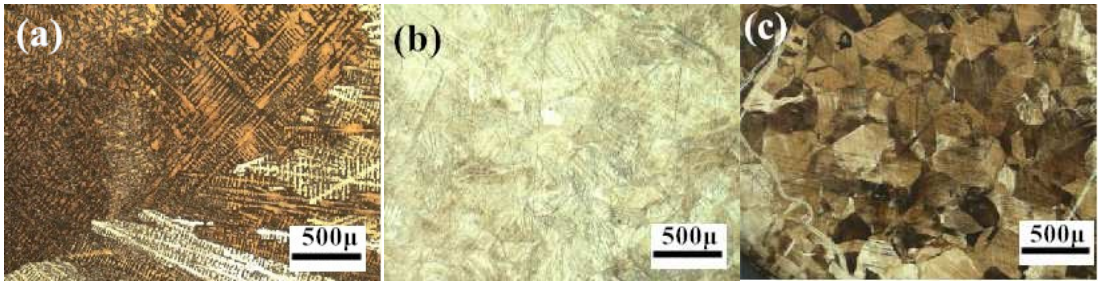

Figure 2. *AuNi9 alloy metallographic (a: cast state; b: processed state (deformation rate 90%); c: ageing state (300°C, 0.5h).*

In order to further determine the impact of the heat treatment on microstructure of AuNi9, energy spectrum analysis was performed by using scanning electron microscope. As shown in Figure 3, the microstructures of the alloy are mainly composed of α-Au solid solution and a small amount of Au-Ni phase.

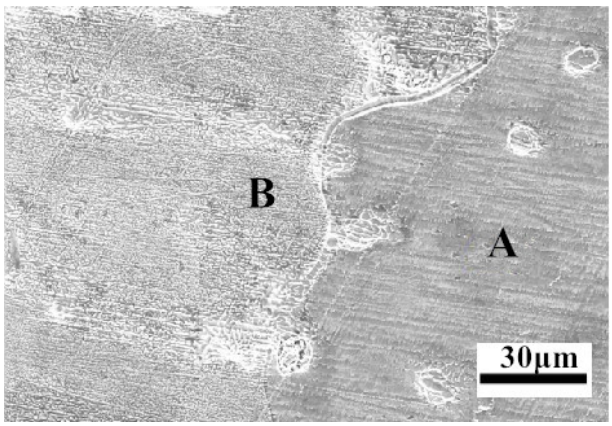

Figure 3. *SEM image of as-cast AuNi9 alloy.*

Table 2. *Chemical analyses at areas shown in Figure 3.*

Symbol	Average chemical analyses, at.%	
	Au	Ni
A	72.84	27.16
B	75.87	24.13

The microstructural image of AuNi9 after heat treatment is given in Figure 4 and the stripe figures are observed. EDS analysis was performed on each area, and the result is shown in in Table 3. The difference in composition causes the depth of metallographic corrosion to be different, thereby forming stripe morphology. The α-Au solid solution decomposes continuously and gradually divides into rich Au and rich Ni.

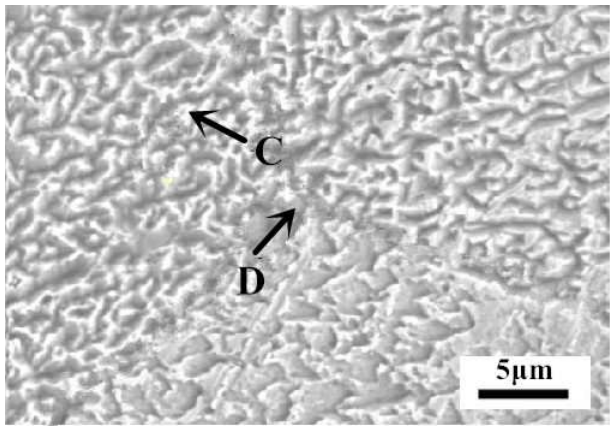

Figure 4. *SEM image of heat treatment AuNi9 alloy.*

Table 3. *Chemical analyses at areas shown in Figure 4.*

Symbol	Average chemical analyses, at.%	
	Au	Ni
C	71.91	28.09
D	75.92	24.08

3.2. Mechanical Properties of AuNi9 Alloy

In order to study the test performance of the alloy after

plastic deformation of the material with different deformation rates, seven deformation rate levels ranging from 0% to 98% were set in the experiment. The trend curves of tensile strength, elongation and Vickers hardness with deformation rate are shown in Figure 5 and Figure 6. It can be seen that the tensile strength continues to increase with the increase of the deformation rate, which is basically a linear increase, while the elongation gradually decreases. This is due to the work hardening caused by dislocation slippage when plastic deformation occurs. The AuNi9 alloy can withstand cold drawing with large deformation rates due to the excellent plastic workability and high strength. When the deformation rate reaches 98%, the strength of the alloy is the highest, which is 1027MPa, and the elongation is the lowest, which is only 0.5%. The hardness is significantly improved, especially before the deformation rate reaches to 70%. When the deformation rate reaches 98%, the hardness of the alloy reaches a maximum of 276HV. Afterward, the growth rate of hardness slows down and gradually tends to remain unchanged.

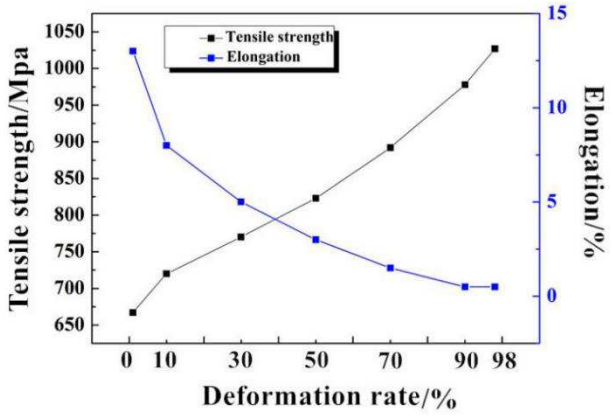

Figure 5. *Tensile properties of samples with different deformation rate.*

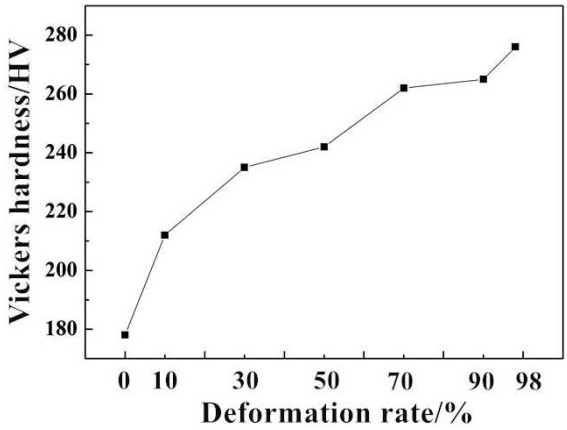

Figure 6. *Vickers hardness for the samples with different deformation rate.*

The hardness test result after heat treatment of the AuNi9 alloy with a working rate of 98% is shown in the Figure 7. It can be observed that the hardness increases significantly at 300°C up to 295 HV due to age strengthening, and then gradually decreases with over-aging. The hardness is basically similar to that of the annealed heat treatment state when the heat treatment temperature reaches to 500°C. The Ni content in the alloy decreases with the heat treatment temperature increases, and the ordered transformation reaches to the upper limit. Therefore, the hardness of AuNi9 alloy decreases because of the recrystallization occured during overaging.

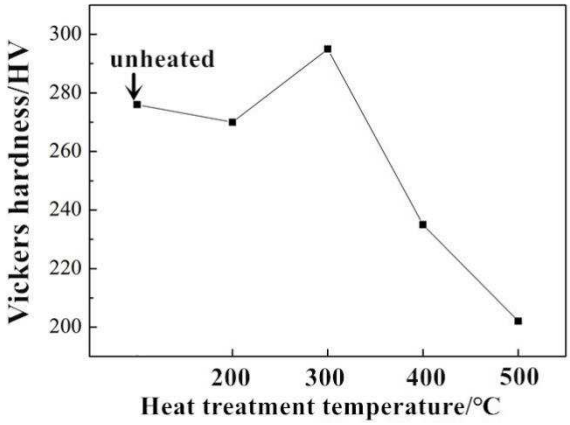

Figure 7. *Vickers hardness for the sample with 98% deformation rate under different heat treatment temperature.*

The effect of holding time at 300°C on the hardness of AuNi9 alloy is shown in Figure 8. It can be seen that there was no obvious change of hardness after heat treatment at 300°C for 15 min compared with normal state. It's said that there is no medium for heat transfer in a vacuum environment, and the alloy fails to reach to 300°C within 15 min [15]. When the holding time reaches 30 min, the hardness of the material increases due to aging strengthening and reaches 290HV. However, the aging strengthening effect is not obvious with the extension of the holding time. Therefore, the optimum holding time is 30 min in order to improve efficiency and reduce oxidation of alloy surface.

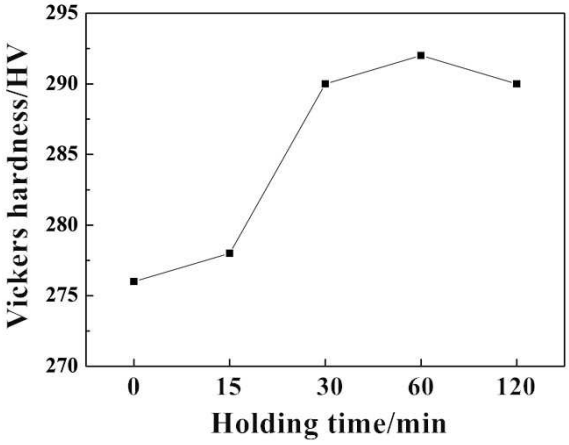

Figure 8. *Vickers hardness for the samples heat-treated at 300°C for different holding time.*

4. Conclusions

In this paper, a systematic study of the corresponding relationship between the alloy preparation process, material

properties and microstructure is carried out to provide a theoretical basis for formulating the optimal process route. The effects of working rate and heat treatment process on the microstructure and properties of the AuNi9 alloy were investigated. Primary conclusions are summarized as follows.

The as-cast microstructure of AuNi9 is mostly consist of dendrite, and the processed microstructure is dominated by twinning. No obvious change of microstructure is observed after heat treatment.

The tensile strength and hardness of AuNi9 increase with the increase of deformation rate, while the elongation decreases. However, the hardness tended to remain changeless when the deformation rate is greater than 50%. The elongation tends to remain unchanged when the deformation rate is greater than 70%.

AuNi9 alloy shows obvious aging strengthening when the heat treatment temperature reaches to 300°C. The hardness of alloy changes little when the holding time exceeds 30min. The optimal heat treatment process is heating at 300°C for 30 minutes.

References

[1] L Shi, S Du, Y Miao, S Lan. Modeling and Performance Analysis of Satellite Network Moving Target Defense System with Petri Nets. Remote Sensing, 2021, 13 (7), 1262.

[2] Z Huang, Q Chen, L Zhang, X HuResearch on Intelligent Monitoring and Analysis of Physical Fitness Based on the Internet of Things. IEEE Access, 2019, 7: 177297-177308.

[3] Jaephil Cho, Sookyung Jeong, Youngsik Kim. Commercial and research battery technologies for electrical energy storage applications, Progress in Energy and Combustion Science, Volume 48, June 2015, Pages 84-101.

[4] S. Ould Amroucheab D. Rekiouab T. Rekiouab S. Bachac Overview of energy storage in renewable energy systems, International Journal of Hydrogen Energy, 2016, 41 (45): 20914-20927.

[5] AH Dida. Design and Modeling of useful Tool for Satellite Solar Array Preliminary Sizing and Power System Analysis. 2019 European Space Power Conference (ESPC), 2019.

[6] Chaoyong Guo, MengZhang, QiangZhang et al. Active control technology for flexible solar array disturbance suppression, Aerospace Science and Technology, 2020, 106: 106148.

[7] Dongzhi Zhang, Yan Yang, Zhenyuan Xu, et al. An eco-friendly gelatin based triboelectric nanogenerator for a self-powered PANI nanorod/NiCo2O4 nanosphere ammonia gas sensor. 2022, 20.

[8] Weijie Shi, Haixia Zhao, Xiaohui Luo. Effect of diamond nanoparticle on the friction Property of sliding friction pair with molecular dynamics simulation, IEEE Access, 2019: 51790-51798.

[9] Da Hai He, Rafael Manory. A novel electrical contact material with improved self-lubrication for railway current collectors. Wear, 2001, 249 (7): 626-636.

[10] Peter Renner, Swarn Jha, Yan Chen, et al. A Review on corrosion and wear of additively manufactured alloys. Journal of Tribology, 2021, 143 (5): 050802- 050820.

[11] WANG Xin-ping, XIAO Jin-kun, ZHANG Lei et al. Effect of load on friction and wear behavior of AuNi9/Au coating tribo-couple, The Chinese Journal of Nonferrous Metals, 2012, 22 (12): 3427-3431.

[12] Li Guo Gang. Study on process of contact material PtIr25 for aeroengine, Chongqing University, China, 2008.

[13] Ueno, T. Kadono, K. Morita, N. Influence of Surface Roughness on Contact Voltage Drop of Elcectrical Sliding. Conrtacts Electrical contacts 2007, the 53rd IEEE holm conference on 2007. 9200-9204.

[14] E. Ogando Arregui, M. Caro, A. Caro. Numerical evaluation of the exact phase diagram of an empirical Hamiltonian: Embedded atom model for the Au-Ni system. PHYSICAL REVIEW B, 2002, 66 (6) 054201-1-10.

[15] ChenpengLiu, YangChen, DailiFeng. Experimental study on temperature uniformity and heat transfer performance of nitrogen loop heat pipe with large area and multi-heat source, Applied Thermal Engineering, 2022, 210 (25): 118344.